ESTIMATING JOINT CARTILAGE THICKNESS ON AN ANIMAL MODEL *ex vivo* USING DIFFUSE REFLECTANCE SPECTROSCOPY

A. Sircan-Kucuksayan [1], M. Canpolat [2*]

[1] *Alanya Alaaddin Keykubat University, Department of Biophysics, Faculty of Medicine, Antalya, Turkey*

[2] *Akdeniz University, Biomedical Optics Research Unit, Department of Biophysics, Faculty of Medicine, Antalya, Turkey; e-mail: canpolat@akdeniz.edu.tr*

A diffuse reflectance visible light spectroscopy method has been developed to estimate bovine cartilage thickness in real time. The system consists of a miniature UV-VIS spectrometer, a halogen tungsten light source, and an optical fiber probe including two 400 μm diameter fibers with a center to center separation of 1.2 mm was used to acquire the spectra. A total of four patellae obtained from bovine just after sacrifice. In the study, ten cattle patella cartilage samples were prepared in a cylindrical shape and thinned by a 200 μm step. Spectra were acquired from the 123 cartilage samples. Cartilage samples were divided into training and validation groups. A correlation between the thickness of the cartilage samples and the absorption spectra was obtained using the data of the training group. The relative thickness of the cartilage was estimated with an average error of 15% in the validation group using the correlation. Diffuse reflectance spectroscopy has the potential to estimate the thickness of cartilage lesions during arthroscopic evaluation of knee cartilages.

Keywords: *cartilage thickness, reflectance spectroscopy, arthroscopy, optical fiber probe.*

ОЦЕНКА ТОЛЩИНЫ СУСТАВНОГО ХРЯЩА НА МОДЕЛИ ЖИВОТНОГО *ex vivo* С ПОМОЩЬЮ СПЕКТРОСКОПИИ ДИФФУЗНОГО ОТРАЖЕНИЯ

A. Sircan-Kucuksayan [1], M. Canpolat [2*]

УДК 535.3:612.751.2

[1] *Университет им. Аладдина Кейкубата Алании, Анталия, Турция*

[2] *Университет Акдениз, Анталия, Турция; e-mail: canpolat@akdeniz.edu.tr*

Разработан метод спектроскопии диффузного отражения видимого света для оценки толщины хряща крупного рогатого скота в режиме реального времени. Для получения спектров использована система, состоящая из миниатюрного УФ-видимого спектрометра, галогенового вольфрамового источника света и оптоволоконного зонда, включающего в себя два волокна диаметром 400 мкм с межцентровым расстоянием 1.2 мм. В общей сложности четыре коленные чашечки получены от крупного рогатого скота сразу после забоя. Подготовлено десять образцов хряща бычьей коленной чашечки цилиндрической формы, истонченных с шагом 200 мкм. Спектры получены из 123 образцов хряща. Образцы хрящей разделены на обучающие и проверочные группы. Корреляция между толщиной образцов хряща и спектрами поглощения получена с использованием данных обучающей группы. При использовании корреляции относительная толщина хряща в группе проверки оценена со средней ошибкой 15%.

Ключевые слова: *толщина хряща, отражательная спектроскопия, артроскопия, оптоволоконный зонд.*

Introduction. Cartilage damage occurs as a result of changes in the molecular composition of the extracellular matrix (EMC). The functionality of cartilage strongly depends on the constitute of its molecular composition. The EMC of cartilage consists of collagen (10–30% wet weight), chondrocytes (10% wet weight), proteoglycans (3–10% wet weight), and water (60–85%) [1]. Cartilage defects that occur with changes in the molecular composition are associated with significant loss of mechanical function and decrease in thickness of the cartilage. The stages of cartilage defects are as follows: softening with the intact group, fibrillations within the superficial layer, cleft down to the subchondral bone, and complete loss of cartilage [2]. Knee cartilage damage assessment during arthroscopy is based on visual examination according to the International Cartilage Repair Society (ICRS) or the Oswestry Arthroscopy Score (OAS) grading systems. Inter-observer reliability of the arthroscopic grading of cartilage lesions is poor [3]. Therefore, orthopedic surgeons need to quantify arthroscopic methods for more effective diagnosis of the lesions [4].

A real-time cartilages assessment based on variations in biochemical compositions may be used as a viable tool in the diagnosis of cartilage deformation due to diseases such as osteoarthritis. Spectroscopic methods have started to be used in recent years for the diagnosis of diseases [5–7]. Several spectroscopic techniques such as near-infrared spectroscopy [8–10] (NIR), optical coherence tomography [11], and Raman spectroscopy [12] were developed to define early stage cartilage degenerations assessing molecular compositions. A correlation between the NIR data and cartilage thickness has been shown by Afara et al. [10]. Traumatic and degenerative cartilage lesions have been distinguished using NIRS in a clinical study [13], and in another study cartilage degeneration was also investigated using NIRS [14]. In the detection of initial cartilage lesions, magnetic resonance imaging (MRI), arthroscopy, and NIRS were used together, and it has been shown that MRI and arthroscopy have low predictive value and that NIRS has potential to be used in the detection of initial cartilage damage [15]. Recently, diffuse reflectance spectroscopy has been employed to assess the cartilage thickness using an optical fiber probe consisting of one source fiber surrounded by six detector fibers [16]. An optimum source-detector fiber separation was defined in diffuse reflectance spectroscopy (DRS) study in the assessment of cartilage thickness on cattle patella [17].

In this study, we have utilized the DRS technique with an optical fiber probe consisting of one source fiber and one detector fiber to estimate cartilage thickness of cattle patella *ex vivo*.

Experimental. *Sample preparation and spectroscopic system.* A total of four patellae obtained from four adult cattle were used in the study. All the patellae were stored at –80ᵒC for 1 day before the experiment. A cylindrical saw with a diameter of 1 cm was used to prepare 10 samples for the spectroscopic measurements. All the samples were cylindrical. The thickness of all undamaged cartilage samples was measured using a digital micrometer and it was found that the range was between 900 to 2150 μm. The first spectrum was acquired from the undamaged cartilage for each sample. Then each cartilage was thinned 200 μm using a microtome; then the spectra were obtained by placing the optical fiber probe on the same place on the cartilage. If the cartilage thickness was less than 200 μm, the cartilage was thinned 100 or 50 μm. The last spectrum was acquired from the bone surface. In total 123 samples were obtained, and eight spectra were acquired from each of them. The average of the eight spectra was used to estimate the cartilage thickness. The samples were divided into two groups, the first one was the training (seven samples) and the second one was the validation (three samples).
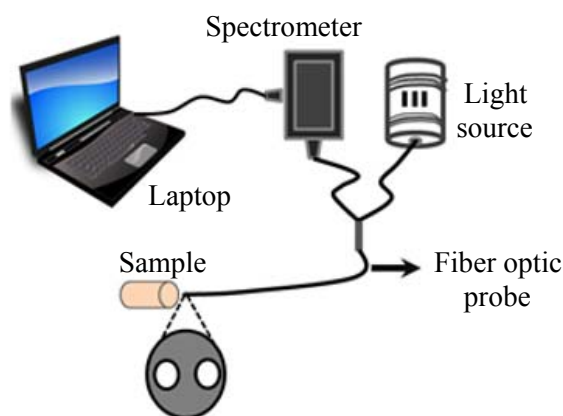

Fig. 1. Schematic view of the system.

The measurement system consists of a halogen tungsten light source (DH2000, Ocean Optics, FL, USA), a miniature spectrometer (USB2000, Ocean Optics, FL, USA), laptop, and a home-made optical fiber probe with two optical fibers with a core diameter of 400 μm. One of the fibers was used to deliver light to the cartilage surface; the other one was used to pick up back reflected light on the same surface. The center-to-center separation of the fibers was 1.2 mm based on our previous study, where the best correlation between the absorption of the hemoglobin in subchondral bone and the cartilage thickness was obtained for the 1.2mm among six source-detector fiber separations [15]. A schematic view of the system is given in Fig. 1.

Spectral data acquisition. Before the spectroscopic measurements on the cartilage samples the system was calibrated. In the calibration process, the first measurement (I_{bg}) was the background signal obtained when the light source was off and the probe on the sample. The second spectrum (I_{spec}) was the back-reflected light from Spectralon (WS-1, Ocean Optics, FL, USA), which reflects the entire wavelength range equally by 99%. The spectrum of the Spectralon was used to eliminate the light source spectral distribution on the measured cartilage spectra. Spectra taken on the cartilage (I_{mes}) were corrected using the equation [17]

$$I(\lambda) = [I_{mes}(\lambda) - I_{bg}(\lambda)]/[I_{spec}(\lambda) - I_{bg}(\lambda)]. \tag{1}$$

The corrected diffuse reflectance spectrum ($I(\lambda)$) provides information on the scattering and absorption of the light within the cartilage and the subchondral bone. Eight spectra were acquired from the cartilage for each thickness. The average corrected spectra over eight measurements for each thickness is used in data analysis presented in Fig. 2a. Optical density from the corrected spectra is defined as

$$OD(\lambda) = \ln(1/I(\lambda)). \tag{2}$$

The valley on the optical density between the wavelengths of 500–600 nm due to hemoglobin absorption gets deeper with smaller cartilage thickness in Fig. 2b. The optical density represents both absorption and scattering of the light within the tissue. Hence, the optical density has two components, absorption $OD_a(\lambda)$ and scattering $OD_s(\lambda)$. Therefore $OD(\lambda)$ can be written as

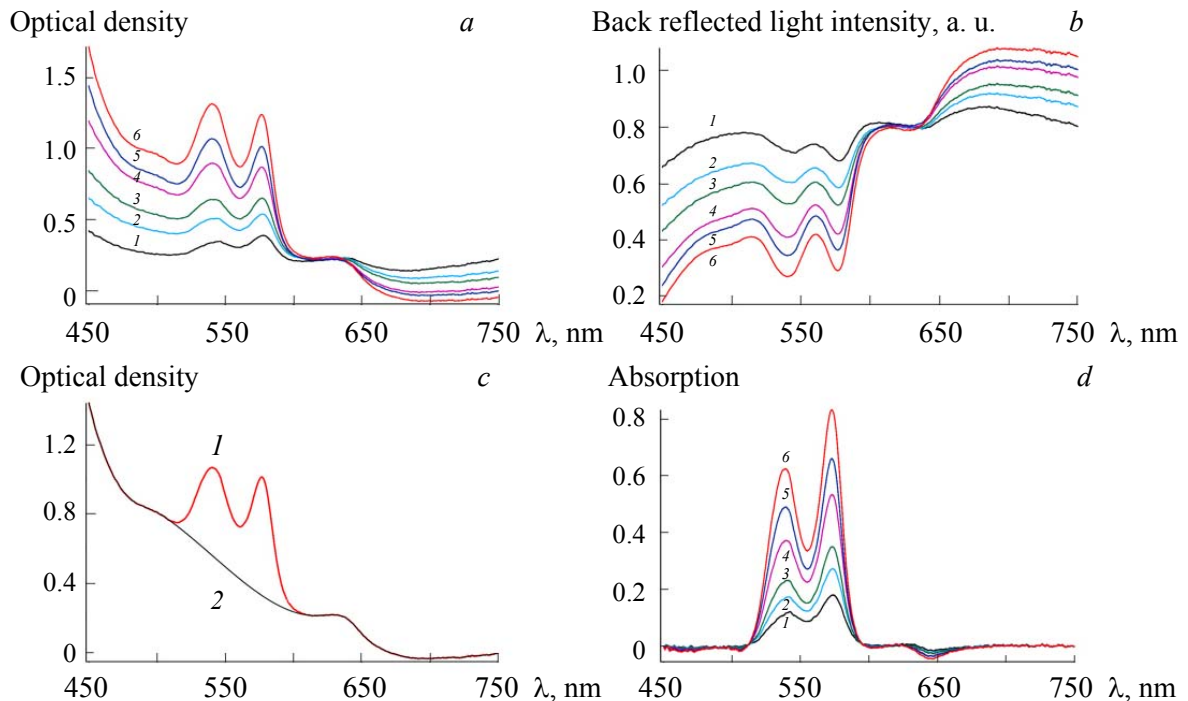$$OD(\lambda) = OD_a(\lambda) + OD_s(\lambda). \tag{3}$$

Fig. 2. (a) Corrected and normalized spectra taken on the cartilage with thickness of 1000 (1), 800 (2), 600 (3), 400 (4), 200 (5), and 0 μm (6), (b) optical density obtained from the back reflected light, (c) optical density data removed in the wavelength range of 510–610 nm (1) and interpolated to the rest of the data (2), (d) absorption spectra of the cartilages with thickness of 1000 (1), 800 (2), 600 (3), 400 (4), 200 (5), and 0 μm (6).

The intensity of the scattered light from the cells changes with $\mu_s'(\lambda)$, which has a power-law dependence on λ [18]. Removing the contribution of the scattering to the optical density gives the pure absorption spectrum of the light in the tissue. The optical density data in the wavelength range of 510–610 nm was removed, and the rest of the data was interpolated using a cubic spline method. The interpolated data are overlapped on the optical density, as seen in Fig. 2c. Then the contribution of the scattering to the optical density was removed by subtracting the interpolated data $OD_s(\lambda)$ (curve 2) from the total optical density $OD(\lambda)$ (curve 1) to obtain the absorption component of the optical density $OD_a(\lambda)$ in Fig. 2d. Absorption of the light increases with decreasing thickness of the cartilage due to the increased optical path length of the light in the subchondral bone, as seen in Fig. 2d. For thick cartilage, a small fraction of the optical path length crosses the subchondral bone, and it increases with decreasing cartilage thickness. If there is no cartilage on the sample, all the light travels in the subchondral bone and the absorption of the light becomes maximum.

Model. Absorption of the light by hemoglobin depends on two parameters. The first is the blood concentration in the subchondral bone. The second one is the optical path length of the light in the subchondral bone. Therefore, we define the absorption of the light by the hemoglobin as

$$A(\lambda) = \varepsilon(\lambda)cd, \tag{4}$$

where $\varepsilon(\lambda)$ is extinction coefficient of hemoglobin, c is the hemoglobin concentration, and d is the optical path length of the light in the subchondral bone. For the same bone, absorption of the light only changes with the optical path length d, and it increases with decreasing cartilage thickness (s). Therefore, the optical path length should be a function of the cartilage thickness ($d = f(s)$). The absorption ratio of undamaged (u) to damaged (d) cartilage is

$$R_A = \frac{A_u(\lambda)}{A_d(\lambda)} = \frac{\varepsilon(\lambda)cf(s_u)}{\varepsilon(\lambda)cf(s_d)} = \frac{f(s_u)}{f(s_d)}. \tag{5}$$

The absorption ratio R_A is obtained for the seven samples in the training set. The ratio is small at small s_d and becomes 1 when s_d equals s_u, as seen in Fig. 3, where the solid line is the average over the seven samples, and the dot lines denote the standard deviation in the training set.

The correlation between the R_A and the relative cartilage thickness (S_d/S_u) is defined in Fig. 3 as

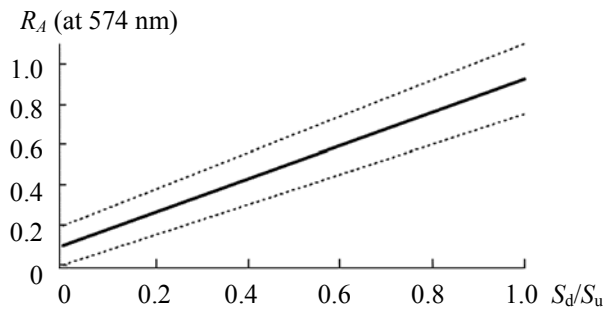$$R_A = 0.926(S_d/S_u) + 0.097. \tag{6}$$

Fig. 3. Absorption ratio of undamaged cartilage to damaged cartilages R_A increases as cartilage damage decrease. The solid line is the average slope over seven cartilages in the training set, and the two dot lines show standard deviation.

Results and discussion. Data of the three cartilages in the validation set were used to estimate the relative cartilage thickness using Eq. (6). As seen in Fig. 4, data of the first sample in the training set fit Eq. (6) with a linear correlation coefficient $Pr = 0.997$. For each sample, actual and estimated thickness, errors, and relative thickness are given in Table 1. Minimum, maximum, and average errors with their standard deviation (SD) over the three samples are 1.5, 18.1, and 7.31±4.37% (mean±SD), respectively.

Grading of the cartilage damage is based on arthroscopic visual examination. Therefore, inter-observer reliability is poor [2]. Diagnosis of cartilage lesion should be in real time, sensitive and reproducible for an effective treatment. One of the lesion assessment methods is measuring the cartilage thickness using quantitative ultrasound imaging (QUI) [19, 20]. However, *in vivo* application of QUI faces some drawback. In the

quantitative measurement, ultrasound should enter the cartilage perpendicularly but, these conditions may not be met in clinical application. Therefore, reflection measurements may change with the implementation of the ultrasound in the clinical setting and need further investigations [12].

In the presented study, we have developed a spectroscopic method to assess cartilage damage by measuring the decrease in the cartilage thickness. A fiber optic probe can fit into the arthroscopy channel in a clinical study. The spectroscopic measurements were performed using visible light. All the data were acquired *ex vivo* on the animal patella to test the developed model. The system estimates the relative cartilage thickness with an average error of 7.31±4.37%.
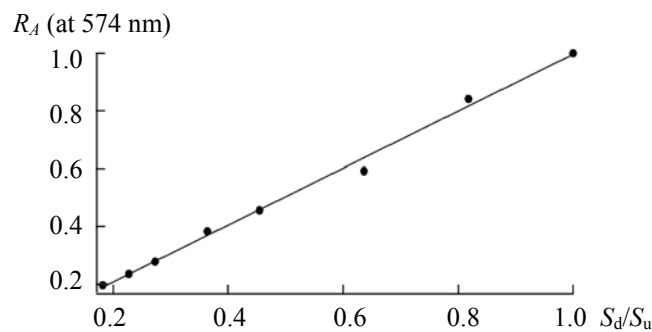

R_A (at 574 nm)

Fig. 4. Data of the first sample in the validation set fit Eq. (6) with linear correlation coefficient $Pr = 0.997$.

TABLE 1. Comparison of Actual and Estimated Cartilage Damages

Cartilage thickness, μm	Relative cartilage thickness (s_d/s_u)	Estimated relative cartilage thickness (s_d/s_u)	Error in the calculated relative cartilage thickness, %
Sample 1			
350	0.304	0.296	2.6
450	0.391	0.401	2.5
550	0.478	0.457	4.4
650	0.565	0.623	10.2
750	0.652	0.534	18.1
950	0.826	0.914	10.7
1150	1	1.062	6.2
Sample 2			
200	0.182	0.174	4.5
250	0.227	0.217	4.6
300	0.273	0.264	3.2
400	0.364	0.379	4.5
500	0.454	0.461	1.5
700	0.636	0.611	4
900	0.818	0.886	8.3
1100	1	1.062	6.2
Sample 3			
250	0.263	0.242	8
350	0.368	0.323	12.2
450	0.474	0.421	11
550	0.579	0.612	5.8
750	0.789	0.711	9.8
850	0.895	1.039	16.1
950	1	1.062	6.2

Variation of the blood perfusion in the bone leads to a change in the absorption independently of the thickness of the cartilage. In the present study, we have aimed to eliminate inter-variability of the blood perfusion in subchondral bone in estimating the cartilage thickness using DRS. Therefore, when measuring the cartilage thickness, we have chosen to use the relative cartilage thickness, defined as the ratio of the thickness of damaged to undamaged cartilage thickness. This approach may reduce the inter-subject variability of the blood perfusion on the spectroscopic measurements.

The blood content of the subchondral bone may be changed during the preparation of the samples using a cylindrical saw due to the high heat caused by the friction between the bone and the saw. Therefore, the correlation defined in Eq. (6) between the cartilage thicknesses and the absorption may not be consistent with the *in vivo* measurements. Currently, we are conducting a clinical study acquiring data from the cartilage lesions *in vivo* in open knee surgeries to obtain a correlation between the absorption and the cartilage thickness. The outcome of the clinical research may bring the possibility of using the developed spectroscopic method in conjunction with nuclear magnetic resonance therapy, which has started to be used for the treatment of cartilage [21] and for follow up of cartilage regeneration.

Conclusion. The existence of a correlation between the cartilage thickness and DRS measurements has been shown. A similar correlation may be obtained acquiring the DRS spectra on knee cartilage *in vivo* during knee surgery. Thus, DRS may be used in the assessment of knee cartilage damage during arthroscopy and to provide information on the thickness of cartilage to a surgeon in real time.

REFERENCES

1. N. P. Cohen, R. J. Foster, V. C. Mow, *J. Orthop. Sport Phys.*, **28**, No. 4, 203–215 (1998).
2. R. E. Outerbridge, *J. Bone Joint Surg.*, B, **43**, No. 4, 752–757 (1961).
3. G. Spahn, H. M. Klinger, M. Baums, U. Pinkepank, G. O. Hofmann, *Arch. Orthop. Traum. Surg.*, **131**, No. 3, 377–381 (2011).
4. G. Spahn, H. M. Klinger, G. O. Hofmann, *Arch. Orthop. Traum. Surg.*, **129**, No. 8, 1117–1121 (2009).
5. A. Sircan-Kucuksayan, M. Uyuklu, M. Canpolat, *Physiol. Meas.*, **36**, No. 12, 2461–2469 (2015).
6. M. Turhan, N. Yaprak, A. Sircan-Kucuksayan, I. Ozbudak, A. Bostanci, A. Derin, *Laryngoscope*, **127**, No. 3, 611–615 (2017).
7. A. Sircan-Kucuksayan, T. Denkceken, M. Canpolat, *J. Biomed. Opt.*, **20**, 115007 (2015).
8. G. Spaln, H. Plettenberg, H. Nagel, E. Kahl, H. M. Klinger, T. Muckley, *Med. Eng. Phys.*, **30**, No. 3, 285–292 (2008).
9. D. Baykal, O. Irrechukwu, P. C. Lin, K. Fritton, R. G. Spencer, N. Pleshko, *Appl. Spectrosc.*, **64**, No. 10, 1160–1166 (2010).
10. I. Afara, I. Prasadam, R. Crawford, Y. Xiao, A. Oloyede, *Osteoarthr. Cartilage*, **20**, No. 11, 1367–1373 (2012).
11. D. K. Kasaragod, Z. H. Lu, J. Jacobs, S. J. Matcher, *Biomed. Opt. Express*, **3**, No. 3, 378–387 (2012).
12. N. S. J. Lim, Z. Hamed, C. H. Yeow, C. Chan, Z. Huang, *J. Biomed. Opt.*, **16**, 017003 (2011)
13. G. Spahn, G. Felmet, G. O. Hofmann, *Arch. Orthop. Traum. Surg.*, **133**, No. 7, 997–1002 (2013)
14. G. Spahn, H. Plettenberg, M. Hoffmann, H. T. Klemm, C. Brochhausen-Delius, G. O. Hofmann, *Arch. Orthop. Traum. Surg.*, **137**, No. 6, 837–844 (2017).
15. G. O. Hofmann, J. Marticke, R. Grossstück, M. Hoffmann, M. Lange, H. K. W. Plettenberg, *Pathophysiology*, **17**, 1–8 (2010).
16. P. A. Oberg, T. Sundqvist, A. Johansson, *Med. Biol. Eng. Comput.*, **42**, No. 1, 3–8 (2004)
17. M. Canpolat, T. Denkceken, C. Karagol, A. T. Aydin, *Proc. SPIE*, **7890** (2011)
18. J. R. Mourant, J. P. Freyer, A. H. Hielscher, A. A. Eick, D. Shen, T. M. Johnson, *Appl. Opt.*, **37**, No. 16, 3586–3593 (1998)
19. S. Koo, G. E. Gold, T. P. Andriacchi, *Osteoarthr. Cartilage*, **13**, No. 9, 782–789 (2005).
20. F. Eckstein, A. Gavazzeni, H. Sittek, M. Haubner, A. Losch, S. Milz, *Magnet. Reson. Med.* **36**, No. 2, 256–265 (1996).
21. D. Krpan, W. Kullich, *Clin. Cases Miner. Bone Metab.*, **14**, No. 2, 235–238 (2017).